

SEISMIC RESISTANCE OF REINFORCED CONCRETE BEAM-AND-COLUMN ASSEMBLAGES
WITH EMPHASIS ON SHEAR FAILURE OF COLUMN

Koichi MINAMI^I and Minoru WAKABAYASHI^{II}

SYNOPSIS

The main objective of this investigation was to know the elastic-plastic behavior of reinforced concrete assemblages with emphasis on shear failure of column subjected to monotonically increasing and well-defined, alternately repeated horizontal load. The principal variables of the experimental program were (1) the shear span ratio of beam and column, (2) the web reinforcement ratio of column and (3) the axial load ratio. The effects of experimental parameters on the strength, stiffness, ductility, failure mechanism and energy absorbing capacity were carefully studied. An analytical model, based on modified shear-friction theory, was formulated to simulate the behavior of the column and comparisons were made between the calculated and observed behavior.

1. INTRODUCTION

The problem of shear failure mechanism of reinforced concrete columns has been of particular interest in recent years, as the result of considerable damage observed in many reinforced concrete frame buildings due to the 1968 Tokachi-Oki Earthquake and the 1971 San Fernando Earthquake. To be able to predict the lateral deformability of a multistory reinforced concrete moment resistance frame subjected to actions expected in severe earthquake, it is necessary to have a clear understanding of the shear behavior of the columns as individual structural elements. Extensive experimental studies on the shear behavior of column subjected to load reversal have been presented by several researchers.

When the structural elements are combined into subassemblages, the interactions taking account of beam elements have to be studied. However, little information is available on the hysteretic behavior of reinforced concrete beam-and-column assemblages with emphasis on shear failure of column. In order to obtain the quantitative informations regarding the elastic-plastic hysteretic behavior of assemblages, experimental investigation of a simple structural subassemblage, a column with two beams framing into it, was carried out.

- Emphasis is placed on the investigation of the following problems.
- (1) Prediction of the column behavior and its significance with respect to shear strength, stiffness and ductility of the assemblage.
 - (2) Influence of the flexural behavior of beam element effect on the lateral deformability of the assemblage.
 - (3) Energy absorbing capacity, which can be estimated by inspection of the hysteresis loops of the assemblage.
 - (4) Research for the simplified mathematical model which includes column deformations in the response analysis of structures subjected to earthquake motions.

-
- I. Lecturer of Osaka Institute of Technology, Osaka, Japan
 - II. Professor of Disaster Prevention Research Institute, Kyoto University, Kyoto, Japan

2. EXPERIMENTS

2.1 Outline of Experiments

The total of 32 reinforced concrete beam-and-column assemblages were tested under constant axial load and monotonically increasing and alternately repeated horizontal load. Features of the test specimens are tabulated in Table. Variables chosen of experiments were the shear-span ratio of beam and column, the web reinforcement ratio of column and magnitude of the constant axial load.

In the names of test specimens, the first numerals, 4 or 8, represent the shear-span ratio of beam, l/D_b , (l : beam length, D_b : beam depth) and the second numerals, 3 or 5, represent the shear-span ratio of column, h/D_c , (h : column length, D_c : column depth). The third numerals indicate the amount of web reinforcement of column. The numerals, 3, 4, 6 and 8 correspond to $r_{pw} = 0.28\%$, 0.47% , 0.57% and 0.85% , respectively, where r_{pw} is the ratio of web reinforcement. The last numerals 15 or 30, denote the magnitude of constant axial compression loaded on the column. The numerals 15 and 30 correspond to $n = 0.15$ and 0.30 , respectively, where n is the ratio of applied axial compression, N , to the load carrying capacity of centrally loaded column, N_o .

2.2 Configuration and Dimension of Test Specimens

All the test specimens had the same rectangular cross section of 150mm x 150mm for column and 150mm x 200mm for beam, as is shown in Fig.1. The numbers and the diameters of the longitudinal reinforcements were so chosen that the flexural capacities of beams were larger than that of column. The specimens represented a beam-and-column assemblage between the point of contraflexure above and below a story level, as shown in Fig.2. Anchor blocks were provided on the outside of the beam-to-column connections.

2.3 Materials and Making of Test Specimens

For the longitudinal reinforcement and web reinforcement, deformed bars SD30 (guaranteed yield stress : 30kg/mm^2) with diameter of 10mm for column and 13mm for beam, and round bars SR24 (24kg/mm^2) with diameter of 4.5mm are used, respectively. The used concrete is a mixture of ordinary Portland cement, coarse aggregates and fine aggregates.

2.4 Loading Apparatus

The loading apparatus, as shown in Fig.3, was designed to meet the state of stress in actual beam-and-column assemblage. Referring to Fig.3, the L-shapes parallel supporting loading frame, prevented the rotation, was jointed to test specimen through a roller support, and was jointed, through the universal joints, to a reversible manual oil jack, with which cyclic horizontal load, Q , was introduced to the test specimen. Loading axis of the oil jack was so aligned that it passed through the mid-point of the column, in order to give anti-symmetric bending and shear upon the specimen. Constant axial load, N , was applied on the gravity center of column of the test frame by another manual oil jack.

2.5 Loading Program

The loading program for the tests is shown in Fig.4. Well-defined, cyclic loading was applied to the test specimens by controlling the prescribed amplitude of the horizontal displacement angle, $R (= \delta/h)$, which is calculated from the measured horizontal displacements, δ .

3. RESULTS OF EXPERIMENTS

3.1 General Cracking Pattern

As shown in Fig.5, the pattern of crack development in the column element of assemblages subjected to cyclic loading were, despite the difference in the experimental parameters, such that the diagonal tension cracks were formed first and developed into shear-bond cracks along the longitudinal reinforcements, with the increase in the deformation amplitude and the number of loading cycles, finally to exhibit shear-bond type of column fracture.

3.2 Measured Hysteretic Characteristics

Some sample hysteretic relations between the applied horizontal load, Q , and the relative displacement angle, R , obtained in the tests are shown in Figs.6(a)-(d). Ordinate of the diagrams represents the applied horizontal load and abscissa gives the measured relative displacement angle. It may be noted that these loops have typical reversed S-shapes after the attainment of maximum strength, that rigidity of the frame in the small load range is close to zero, and that the closed area by a loop which is the capacity of energy absorption is very small. Also indicated in the figure is that, as the axial load becomes larger, the maximum strength of the frame increases, but deterioration in load carrying capacity is rather drastic after the frame reaches its maximum strength.

Figure 7 shows the strength reduction when the cyclic loading is applied on the specimen under a fixed value of the displacement amplitude. The strength reduction factor (the ratio of the maximum strength attained in each cycle of loading to the maximum strength in the first cycle under that amplitude) is taken for the ordinate, and the number of loading cycles is taken for the abscissa. In general, the strength reduction factor converges to a certain value after 3 cycles of loading, about 60%.

In Fig.8, the sustained load and the displacement angle at the returning point under each displacement amplitude are plotted in Q - R coordinates. The horizontal load-displacement angle relationships obtained from the companion specimens under monotonic loading is also given in the figure.

3.3 Measured Strength

For each specimen, the measured maximum strength, Q_{max} , and the measured minimum strength, Q_{min} , detected at the negative loading under $R = -0.03rad.$, are plotted in Fig.9. In the figure, Q_{cal} is compared with the maximum and minimum strengths of each specimen, where Q_{cal} is the temporary allowable shear strength of column obtained from AIJ standard.

3.4 Energy Absorbing Capacity

Shown in Figs.10(a)-(c) is the relationship between the magnitude of energy consumed with every half cycle of loading and the number of loading cycles, computed from the hysteresis loops. In the figure, ordinate represents the energy absorbing capacity within every half cycle of loading, U_k , and the accumulated energy absorbing capacity, U , which is obtained from $\sum U_k$. Abscissa represents the numbers of cycles, K . Within the same cycle of loading, the value U_k for the reloaded loops were smaller than that in the virgin loop, and this tendency was, despite the difference of experimental parameter, more clearly seen in the loops of the amplitude of displacement before the attainment of maximum strength.

From Fig.10(a), it is observed that the accumulated energy absorbing capacity was significantly improved by the increasing the amount of web reinforcement after the attainment of maximum strength. It seems from Fig. 10(b) that the accumulated energy absorbing capacity obtained in the test increases with the increases of the amount of axial load. On the other hand, the flexural rigidity of beam has significant effect on the accumulated energy absorbing capacity before the attainment of maximum strength, as shown in Fig.10(c).

4. ANALYTICAL MODEL

As already indicated, the shear-bond failure mechanism of column play a key role to determine the measured hysteretic behavior of the beam-and-column assemblages. An analytical model of failure mechanism of column, based on the modified shear-friction theory, was developed to simulate the observed behavior of column. The assumed shear-carrying mechanism of the column after the formation of the shear-bond crack is shown in Fig.11. An important feature of the idealization is related to the shear resistance of the potential shear-bond crack, and the flexural resistance of confined concrete under applied constant axial load.

As is shown in a free body diagram, the magnitude of the transfer shear stress, τ , to slip displacement, s , of confined concrete, considered to be a function of slip displacement, is given by

$$\frac{F}{b \cdot h} = \tau(s) = \alpha \cdot F_c \frac{b'}{b} + \beta \cdot r \rho_w \cdot r_w \sigma_y$$

where αF_c is a possible apparent cohesion stress and β is the coefficient of friction (F_c : concrete strength, $r_w \sigma_y$: the yield stress of web reinforcement, b : column width, b' : shear transfer width). The approximation used in this investigation for the relationship between the shear stress and slip displacement given in Fig.12. In the figures, actual response of shear transfer, obtained from push-pull-off test specimen by the author, is illustrated by the dotted line.

Considering the geometrical condition, $s = \frac{d'}{2} \phi$ (d' : distance between upper and lower main reinforcing bar, ϕ : rotation angle of a column), the computed hysteretic response for column can be expressed by

$$Q = \frac{N \cdot d'}{h} \left(1 - \frac{N}{b \cdot d' \cdot \sigma_c} \right) - N \cdot \phi + b \cdot d' \cdot \tau(\phi)$$

in which σ_c = compressive stress of confined concrete, as a function of rotation angle of a column.

An example of calculated hysteresis loops for the beam-and-column assemblage involved the flexural deformation of beams and column is shown in Fig.13. Figure 13 also shows the measured hysteresis loops in the first circle under each displacement amplitude. The agreement between the measured and calculated maximum strength is satisfactory, but the shape of the calculated hysteresis loop does not exactly exhibit the rate of stiffness and strength degradation observed in the measured hysteresis loops.

5. CONCLUSIVE REMARKS

Stated above is the observed and calculated hysteretic characteristics of reinforced concrete beam-and-column assemblages with emphasis on shear-bond failure of column. It is hoped that the analysis suggested herein will be helpful in stimulating analytical and experimental studies which will lead eventually to the rigorous rational solution.

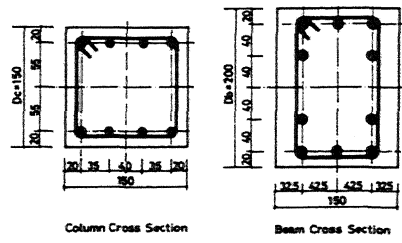


Fig. 1 Details of Cross Section

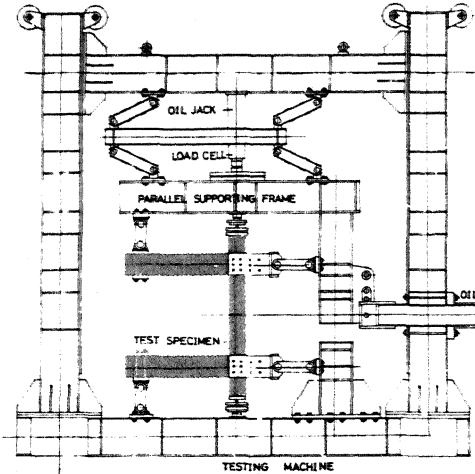


Fig. 3 Loading Apparatus

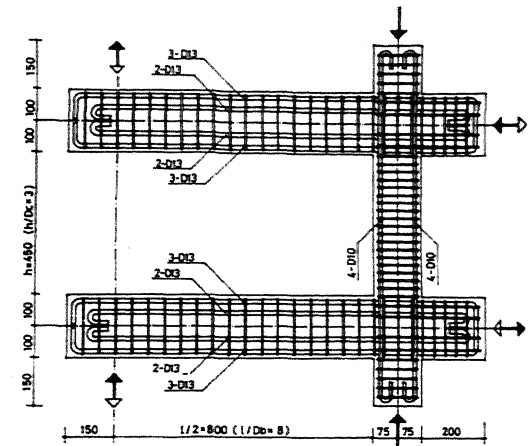


Fig. 2 Dimensions and Arrangement of Reinforcements, Specimen 83830R

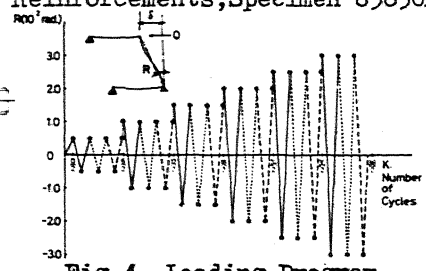


Fig. 4 Loading Program

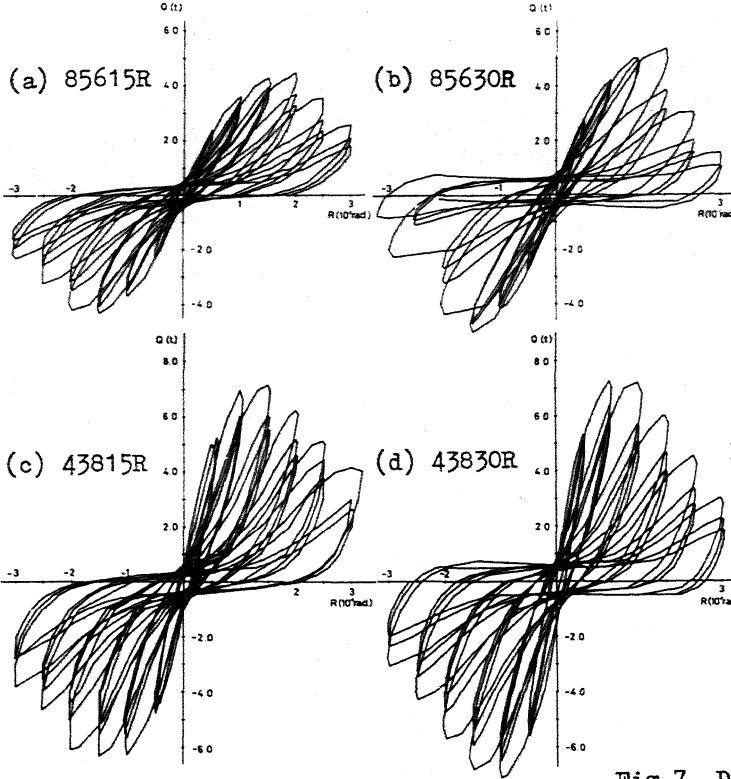


Fig. 6 Load-Deflection Relationships

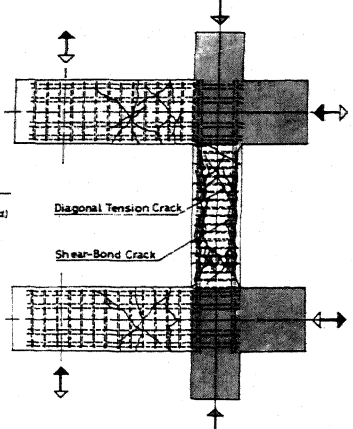


Fig. 5 Crack Observation, Specimen 43830R

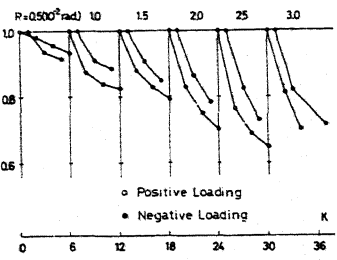


Fig. 7 Deterioration of Strength, Specimen 83815R

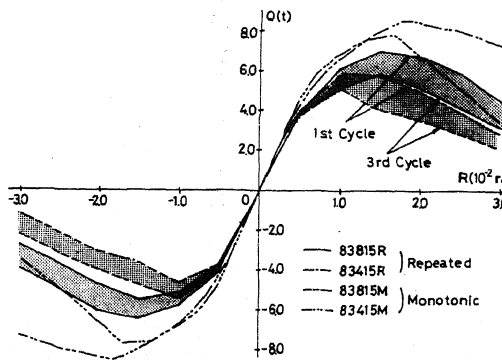


Fig. 8 Effect of Cyclic Loading

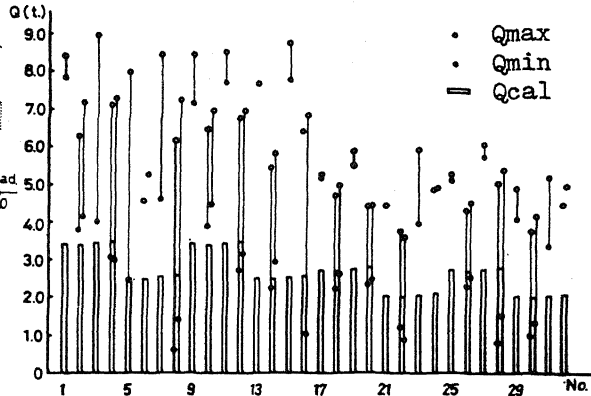
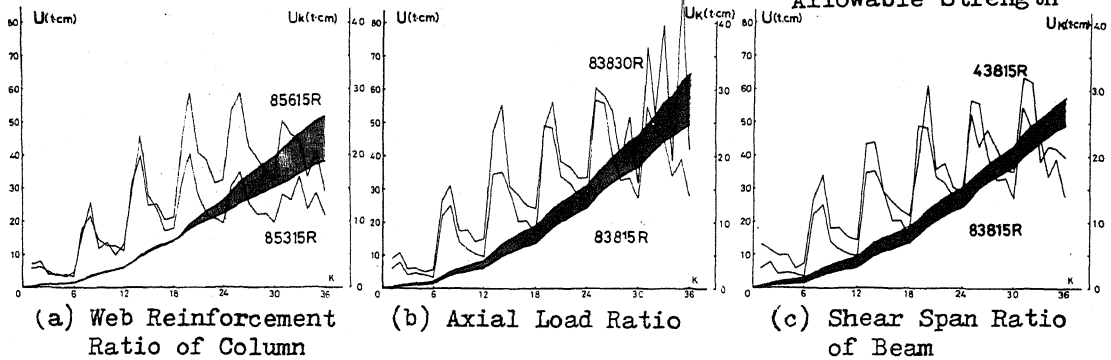


Fig. 9 Comparison of Measured and Allowable Strength



(a) Web Reinforcement Ratio of Column

(b) Axial Load Ratio

(c) Shear Span Ratio of Beam

Fig. 10 Energy Absorbing Capacity

Table Test Program

No.	Specimen Name
1	4 3 8 1 5 M
2	4 3 8 1 5 R
3	4 3 8 3 0 M
4	4 3 8 3 0 R
5	4 3 4 1 5 M
6	4 3 4 1 5 R
7	4 3 4 3 0 M
8	4 3 4 3 0 R
9	8 3 8 1 5 M
10	8 3 8 1 5 R
11	8 3 8 3 0 M
12	8 3 8 3 0 R
13	8 3 4 1 5 M
14	8 3 4 1 5 R
15	8 3 4 3 0 M
16	8 3 4 3 0 R
17	4 5 6 1 5 M
18	4 5 6 1 5 R
19	4 5 6 3 0 M
20	4 5 6 3 0 R
21	4 5 3 1 5 M
22	4 5 3 1 5 R
23	4 5 3 3 0 M
24	4 5 3 3 0 R
25	8 5 6 1 5 M
26	8 5 6 1 5 R
27	8 5 6 3 0 M
28	8 5 6 3 0 R
29	8 5 3 1 5 M
30	8 5 3 1 5 R
31	8 5 3 3 0 M
32	8 5 3 3 0 R

M: Monotonic
R: Repeated

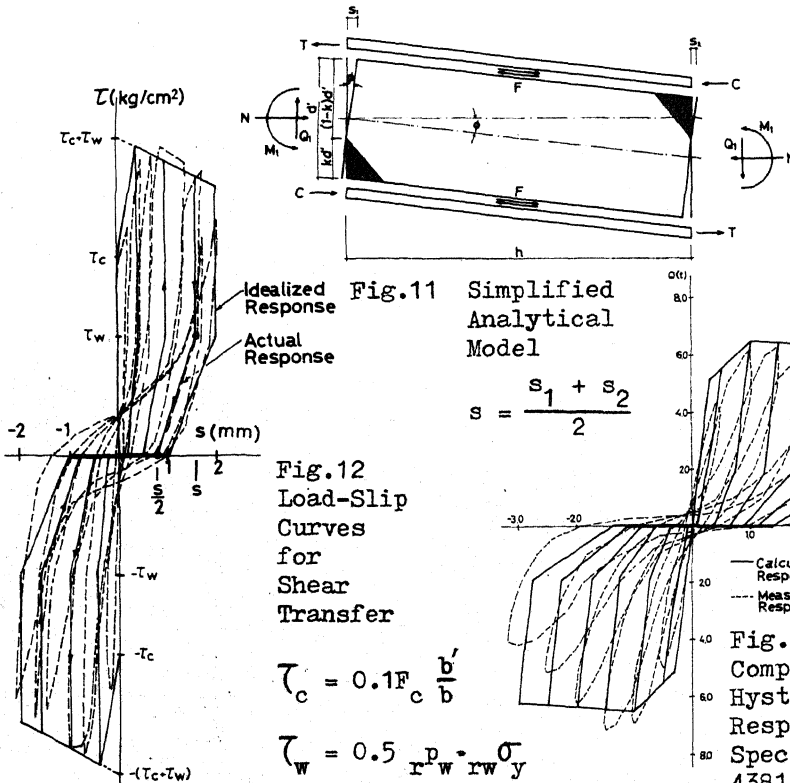


Fig. 11 Simplified Analytical Model

$$s = \frac{s_1 + s_2}{2}$$

Fig. 12 Load-Slip Curves for Shear Transfer

$$\tau_c = 0.1 F_c \frac{b'}{b}$$

$$\tau_w = 0.5 r_w^p \cdot r_w \cdot \sigma_y$$

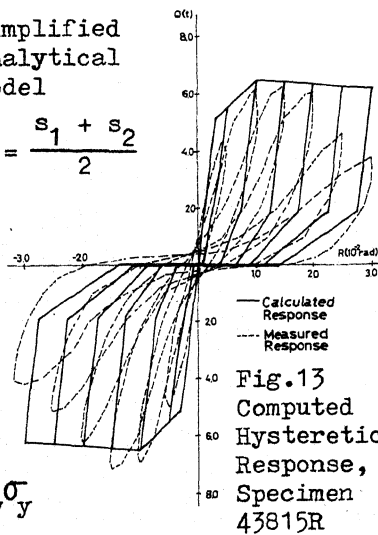


Fig. 13 Computed Hysteretic Response, Specimen 43815R